17th Brazilian Congress of Thermal Sciences and Engineering
November 25th-28th, 2018, Águas de Lindóia, SP, Brazil

ENCIT-2018-0774
MATHEMATICAL MODEL FOR OPTICAL LOSSES CALCULATION IN HELIOSTAT FIELDS IN SOLAR TOWER POWER PLANTS

Matheus Protásio de Lima
Gabriel Ivan Medina Tapia
Universidade Federal do Rio Grande do Norte, Campus Universitário, Departamento de Engenharia Mecânica, Laboratório de Sistemas Térmicos e Energias Alternativas – LSTEA, Lagoa Nova. CEP: 59072-970. Natal-RN, Brasil.
matheus.protasio@bct.ect.ufrn.br; gmedinat@ct.ufrn.br

Abstract. *This study aims to develop a mathematical algorithm to simulate the heliostat field behavior in solar tower power plants in order to estimate the optical loss mechanisms of these systems and consequently to assist in new projects design. The loss mechanisms calculated in the code are reflectivity, cosine effect, atmospheric attenuation, spillage, blocking and shadowing; according to the geographical location of the plant and the mirrors arrangement in the field. In result, it is performed a case study investigating different configurations in fields located at low latitudes: a circular layout a southern layout, which have achieved an annual efficiency of 67.0% and of 60.3%, respectively.*

Keywords: *Optical Losses, Heliostat Field, CSP, Solar Tower Plant, Mathematical Algorithm*

1. INTRODUCTION

In today's world, energy is directly linked with a number of global challenges such as climate changes, conflicts between nations, world economic stability, and food security. Therefore countries around the world are increasingly investing in new technologies for the production of clean and renewable energy. In this context, solar energy has played an important role in complementing the world's energy demand and, subsequently, contributing to fossil fuels replacement.

Concentrating solar power (CSP) systems, such as parabolic trough collectors, Fresnel collectors, solar dish collectors and central receiver systems (solar tower power plants) are promising sources of clean energy.

Concentrating solar power (CSP) is an electricity generation technology that uses heat provided by solar irradiation concentrated on a small area. Using mirrors, solar energy is reflected into a receiver where heat is collected by a thermal energy carrier and subsequently used to generate electrical energy power in a turbine or other thermal engine. (Wagner, 2008).

Solar power tower technology has a considerable advantage over other CSP systems due to its ability to achieve high operating temperatures, resulting in greater power cycle efficiencies (Besarati, 2014). This technology is a concentrating solar energy application that produces electrical energy using solar radiation fluxes in high concentration - about a thousand times the average solar radiation - that are reflected by large mirrors (heliostats) on a receiver located on top of a tower. A heat transfer fluid (HTF) is used to absorb the thermal energy of the receiver and can be used to generate electricity in traditional cycles such as Rankine and Brayton (Wagner, 2008). A solar tower power plant is shown in Fig. 1.

The main focus of this study will be the heliostats field which represents a key subsystem in solar power towers because it normally contributes about 50% to the total plant cost and accounts for 40% of the power losses (Collado and Guallar, 2012b). Therefore the use of computational programs that calculate the loss mechanisms of these systems in an efficient way achieve great interest to optimize the design of the solar plants.

Regarding the solar resource, CSP technology is particularly indicated in regions with high values of Direct Normal Irradiance (DNI). DNI is an essential component of global irradiance and represents the amount of irradiation received from the sun without having been scattered by the atmosphere and focused on a plane normal to the sunlight direction (Blanc *et al*., 2014).

In this work, a computational algorithm is developed that applies mathematical methods to estimate the loss mechanisms present in heliostats field of solar tower power plants. The main objective of this study is investigate the behavior of distinct heliostat field configurations at low altitudes. Therefore, the algorithm estimates the field efficiency and, consequently, the predict power generation.

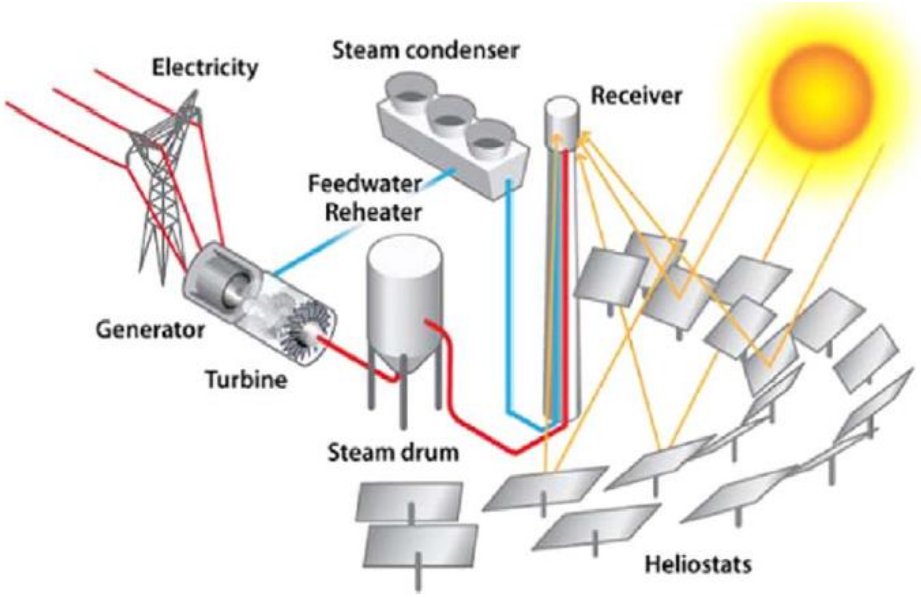

Figure 1. Schematic diagram of solar tower or central receiver system (Purohit and Purohit, 2017)

After estimating the efficiency and the instant power for all the time intervals over a year, it is possible to identify the annual energy production for a solar tower plant and indicate the feasibility of new plants installation for electric power generation.

The authors believe that studies such as this paper have great importance to enable the CSP energy generation in some regions of the Brazilian northeast that have high DNI incidence (over 2000 kWh/m²year), such as the western mesoregion of Rio Grande do Norte.

2. METHODOLOGY

The algorithm described in this work was developed in MATLAB and uses some functions of this platform in order to calculate some processes described in the literature.To simulate the behavior of the heliostats field in central tower plants, this work is divided into two parts: the first describes the calculations necessary to know the relative position of the sun for each day and time in a geographic position chosen for the installation of the plant; the second calculates the loss mechanisms for a predefined layout heliostat field.

2.1 Relative position of the sun

Conventionally, two angles are used to define the apparent movement of the sun relative to the earth's surface: solar height (α) and azimuth angle (γ). The value of these angles are functions of the geographical position of the observer, with respect to its respective latitude and longitude, in addition to the day and time of observation. The equations for describing the solar height and azimuth angles used in the code were taken from Duffie and Beckham (2013).

To obtain the solar height and azimuth angles, the program calculates other parameters through the day and time values. First, the Eq. (1) calculates the Declination, i.e., the angular position of the sun at noon with respect to the equatorial plane.

$$\delta = 23.45 \sin\left(360 \cdot \frac{284 + n}{365}\right) \tag{1}$$

where n is the day of year.

Then, Eq. (2) calculates the hour angle (ha), which is used to correct the time effect on the local meridian.

$$ha = 15\left[(h - 12) + (m/60)\right] \tag{2}$$

where h is the current hour and m is the current minute.

Finally, after calculating these two angles and knowing the latitude (ϕ), it is possible to calculate the solar height by Eq. (3) e and the azimuth by Eq. (5). The Equation (4) calculates the Zenith angle (θ_z), in degrees, that is used in Eq. (7).

$$\sin(\alpha) = \sin(\delta)\sin(\phi) + \cos(\delta)\cos(\phi)\cos(ha) \tag{3}$$

$$\theta_z = 90 - \alpha \tag{4}$$

$$\gamma = sign(\omega)\left|\arccos\left(\frac{\cos\theta_z \sin\phi - \sin\delta}{\sin\theta_z \cos\phi}\right)\right| \tag{5}$$

2.2 Heliostat field configuration

In the literature, several algorithms have been proposed to improve heliostat solar field performance. In this study, radial staggered configuration has been proposed to investigate heliostat field behavior in solar tower power plants. The radial staggered layout was proposed by the University of Houston for the RCELL code and was used for the Solar One Project, a pilot solar-thermal project built in the Mojave Desert, USA (Barberena *et al.*, 2016).

In these layouts the heliostats are located around a tower in rings. The heliostats of a ring are placed with an azimuth angular spacing and the algorithm ensures that no heliostat is in front of other heliostat of an adjacent row (Mutuberria *et al.* 2015). Fig. 3 displays a schematic view of heliostats locations in a radial staggered configuration.

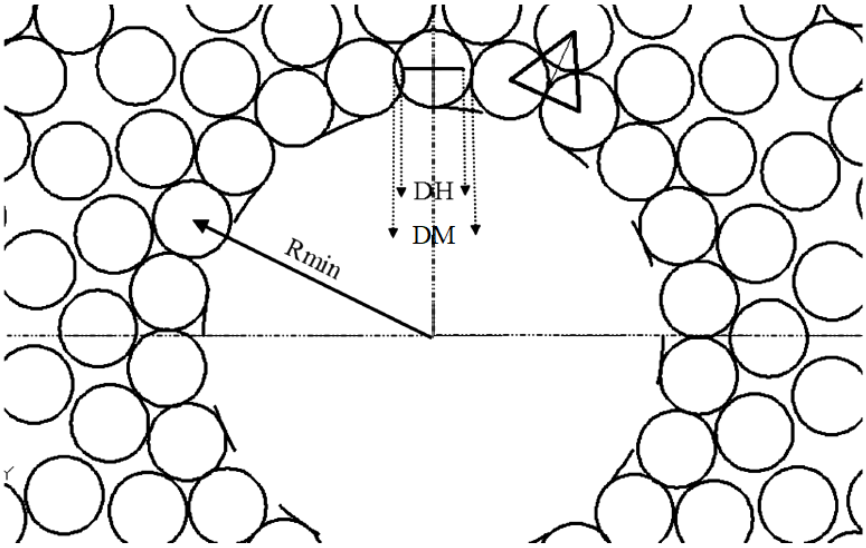

Figure 2. Schematic view of locations of heliostat (Talebizadeh *et al.*, 2014)

The diameter of the heliostat DH (the length of the inner segment in the circles) is given by Eq. (6).

$$\mathrm{DH} = \sqrt{\mathrm{LW}^2 + \mathrm{LH}^2} \tag{6}$$

where LW is the heliostat width and LH is the heliostat height. Then, DH is equal to the heliostat diagonal.

In order to reduce the shadowing and blocking losses, and to keep the minimum distance for mechanical constraints, the algorithm adopted a parameter *dsep* to define the distance between heliostats. Thus, the diameter DM, that is, the diameter of the heliostat plus the security distance is calculated by Eq. (7):

$$\mathrm{DM} = \mathrm{DH} + \mathrm{dsep} \tag{7}$$

To avoid that a heliostat stays in front of other heliostat, the radial staggered algorithms lay out the next row heliostats between the mirrors from front row, as shown in the Fig. 3. R_1 is the distance between the first row and the tower. In this work, it was dsep = 0.2 DH and R_1 values close to 0.82 THT (tower optical height), the reference case studied by Collado and Guallar (2012b).

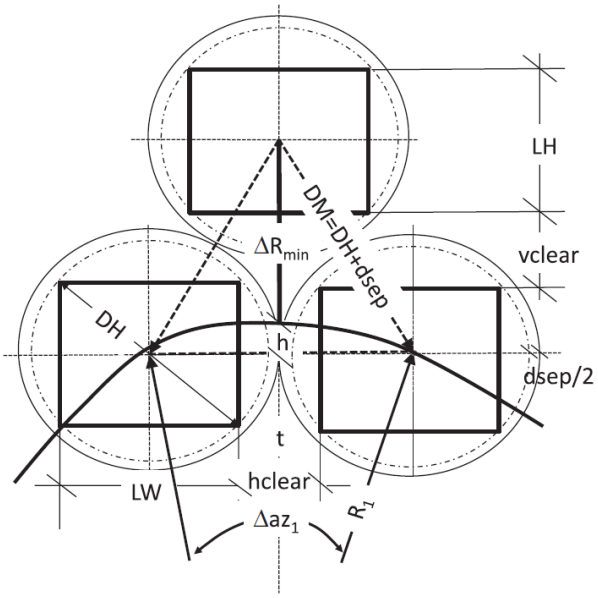

Figure 3. Minimum radial increment, additional separation distance, and vertical and horizontal clearances. (Collado and Guallar, 2012a)

2.3 Loss mechanisms calculation

The optical loss mechanisms are calculated from the different efficiency factors described in Eq. (8). These factors describe the following phenomena: reflectivity, cosine effect, atmospheric attenuation, spillage, blocking and shadowing. Fig. 4 summarizes the way these mechanisms operate in solar tower plants. The calculation of the optical losses efficiency η follows the classic nomenclature of Sandia National Laboratories from USA, described in Collado and Guallar (2012b).

$$\eta(x,y,t) = \rho \cdot \cos\omega(x,y,t) \cdot f_{at}(x,y) \cdot f_{\text{int}}(x,y,t) \cdot f_{s\&b}(x,y,t,\textit{neighbour heliostats}) \tag{8}$$

where ρ is the heliostat reflectivity, $\cos\omega$ the cosine effect, f_{at} the atmospheric attenuation factor, f_{int} the intercept factor (spillage efficiency) and $f_{s\&b}$ is the blocking and shadowing efficiency. Note that some factors depends on the relative position of the heliostats and the field location (x, y) and others are also dependent on solar time (t).

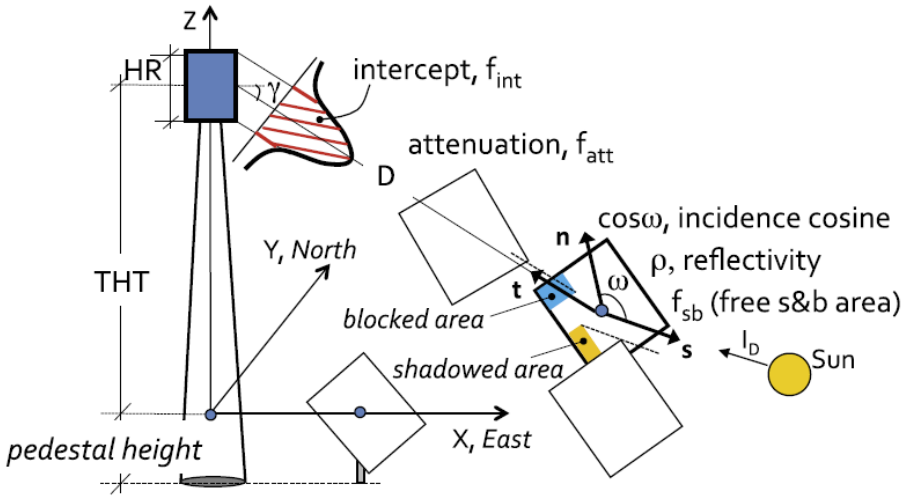

Figure 4. Nomeclature of optical efficiency in heliostat fields (Collado and Guallar, 2012b)

2.3.1 Reflectivity and Sener heliostats

In order to carry out simulations closer to reality, the parameters of Sener heliostats will be used in the code. These mirrors are used in Gemasolar, the first solar power tower commercial plant with molten salt storage. The total dimensions of Sener heliostats have been reported by Collado and Gullar (2012b), namely heliostat height LH=9.752 (m) and heliostat width LW=12.305 (m). Thus, the total area of the heliostat is 120 (m²) and its diagonal DH=15.7 (m).

To estimate the reflectivity losses of the mirrors, the nominal reflectivity of 0.88 will be used plus with the multiplying factor of 0.95 which is a function of the cleaning frequency of the heliostats, which would depend on the plant's maintenance level (Collado and Guallar, 2012b).

2.3.2 Cosine effect

The cosine effect is one of the main losses factors of a heliostat field, being in most cases, the most significant factor. This is the reduction of the effective area reflected by the heliostat due to the angle formed between the solar position vector ($\vec{u}_s$) e the normal heliostat vector ($\vec{n}$). Thus, the incidence cosine is merely the dot product of unitary vectors $\vec{n}$ and $\vec{u}_s$, or $\vec{n}$ and $\vec{u}_t$, the reflected vector from the heliostat point to the receiver. The cosine effect is calculated by Eq. (9):

$$\eta_{\cos} = \cos\omega(x,y,t) = \vec{n}(x,y,t)\cdot\vec{u}_s(location,t) = \vec{n}(x,y,t)\cdot\vec{u}_t(x,y) \tag{9}$$

The unitary solar position vector is calculated using Eqs. (3-7) and is given by Eq. (10) from Ramos and Ramos (2014) with the appropriate coordinate system change.

$$\vec{u}_s = \left[-\cos\alpha\sin\gamma, -\cos\alpha\cos\gamma, \sin\alpha\right] \tag{10}$$

In order to no calculate the normal heliostat vector, this algorithm uses an algebraic strategy described by Kistler (1986), where it is possible to calculate the cosine of 2 times the incidence angle just with $\vec{u}_s$ and $\vec{u}_t$, as it is given by Eq. (11).

$$\cos 2\omega(x,y,t) = \vec{u}_s(location,t)\cdot\vec{u}_t(x,y) \tag{11}$$

2.3.3 Atmospheric attenuation

The atmospheric attenuation factor corresponds to the losses of radiation in the air between the heliostat field and the receiver. This mechanism is simply a function of the distance between the heliostat and the receiver and can be calculated by Eqs. (12-13) according to study of Schmitz *et al.*, (2006).

$$f_{at}(x,y) = 0.99321 - 0.000176D + 1.97\cdot 10E - 8D^2 \quad (D \le 1000\ m) \tag{12}$$

$$f_{at}(x,y) = e^{-0.0001106D} \quad (D > 1000\ m) \tag{13}$$

where D is the distance between heliostat and receiver.

2.3.4 Spillage

Spillage refers to the part of the radiation reflected by the heliostat field that is outside the receptor domain. This loss mechanism can be calculated by integrating the energy flux produced by the mirrors onto the receiver (García *et al.*, 2015). In this work, the mathematical method to calculate the field yield for the spillage (intercept factor) is the HFLCAL model, a program developed by German Aerospace Center (DLR) to optimizing the heliostat fields.

The HFLCAL describes the energy flux density as a circular normal (Gaussian) distribution (see Fig. 4). Thus, the intercept factor can be calculated by integrating the flux along the receiver aperture plane, as shown by Eq. (14):

$$f_{\text{int}}(x,y,t) = \frac{1}{2\pi\sigma_{tot}^2}\int_x\int_y \exp\left(-\frac{x^2+y^2}{2\sigma_{tot}^2}\right) dy\cdot dx \tag{14}$$

Where σ_{tot} is the total standard deviation. This deviation is the result of the convolution of four Gaussian error functions, namely sunshape error (σ_{sun}), beam quality (σ_{bq}), the astigmatic effect (σ_{ast}) and, finally, the tracking error (σ_t). Then, σ_{tot} can be described by Eq. (15):

$$\sigma_{tot} = \sqrt{D^2(\sigma_{sun}^2 + \sigma_{bq}^2 + \sigma_{ast}^2 + \sigma_t^2)} \tag{15}$$

where D is the distance between heliostat and receiver. For σ_{sun} is used 2.51 (mrad), the standard deviation to sunshape measured in PSA, a center for solar energy exploration, situated in Almería, Spain. The standard deviation of beam quality σ_{bq} was obtained after some tests of Sener heliostats and assumes the value of 1.88 (mrad). Also after 240 tracking tests of Sener heliostats under low wind speed conditions, a tracking error σ_t of 0.63 (mrad) has been reported (Collado and Guallar, 2012b). Finally, the standard deviation of the astigmatic effect is described in Eq. (16):

$$\sigma_{ast} = \frac{\sqrt{0.5(H_t^2 + W_s^2)}}{4D} \tag{16}$$

where H_t and W_s are, respectively, the image dimensions in the tangential and sagittal planes at a distance D from the mirror. Their values are calculated by Eqs. (17-18):

$$H_t = DH\left|\frac{D}{f} - \cos w\right| \tag{17}$$

$$W_s = DH\left|\frac{D}{f}\cos w - 1\right| \tag{18}$$

where f is the focal distance, equal to *D* when the heliostat is focused on its slant range as usual.

Concerning to the integration limits in Eq. (15), the intercept factor may be the integral on the contours of the cylindrical receiver for a surrounding field as shown in Fig. 5.

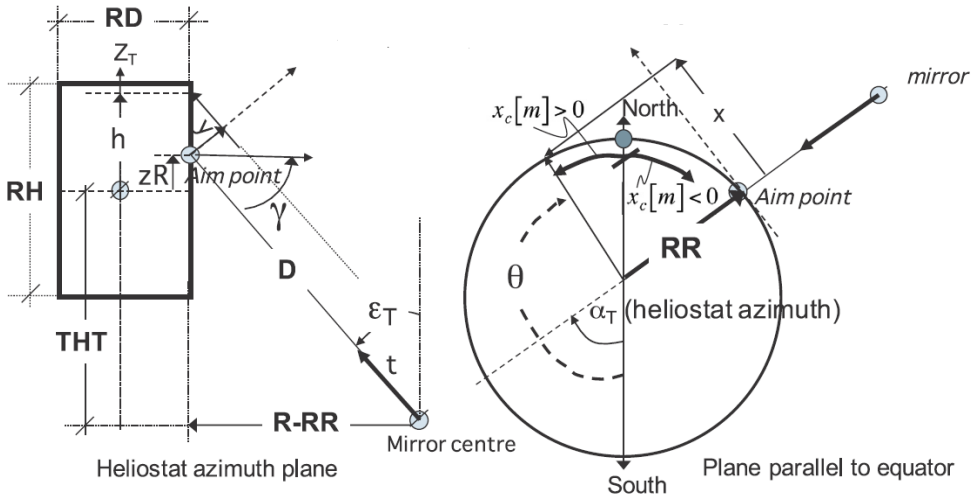

Figure 5. Projection of a point in the image plane on the cylindrical surface (Collado and Guallar, 2018)

Thus, the cylindrical receiver is seen by the heliostat as a rectangle with a width equal to the diameter of the receiver 2 x RR (Receiver Radius), and a height HR x cosγ. HR is the height receiver and γ is the complementary angle of ε_t, that is, the angle between the vector from the heliostat point to the tower and the vertical. The integration of the Eq. (14) is immediate through the error function, as shown by Eq. (19):

$$f_{\text{int}}(x,y,t) = \frac{1}{4}\left(\left(erf\left(\frac{RR}{\sigma_{tot}\sqrt{2}}\right) - erf\left(\frac{-RR}{\sigma_{tot}\sqrt{2}}\right)\right) + \left(erf\left(\frac{RH\cos\gamma}{2\sigma_{tot}\sqrt{2}}\right) - erf\left(\frac{-RH\cos\gamma}{2\sigma_{tot}\sqrt{2}}\right)\right)\right) \tag{19}$$

To calculate the intercept factor in the algorithm, it was used the function *erf* from MATLAB.

2.3.5 Blocking and Shadowing

Blocking and shadowing are considered by the majority of authors as the most difficult loss mechanisms to be modeled computationally, since these factors depend not only on the geographic location of the plant and the instant of time considered, but also on the relative position of neighboring heliostats. In order to estimate blocking, it was used an analytic expression for radial staggered layouts described in Collado (2009)

This analytic expression considers only the two "shoulder" heliostat in the first row in front, and the azimuth of the heliostat normal is the same as that of the unitary vector pointing to the tower from the center of heliostat. Eq. (20) describes the analytic function for blocking mechanism calculation.

$$f_b = 1 - \left[1 - \frac{\Delta R}{LH}\left(\frac{\cos\varepsilon_T + \tan\beta \sin\varepsilon_T}{\cos\omega}\right)\right] \cdot \left[\frac{2wr - \left(\sqrt{1+wr^2} + dsep\right)}{wr}\right] \tag{20}$$

where ΔR is the radial increment between consecutive and staggered rows, wr is the width-height ratio of heliostat and β is the ground slope (for flat terrains, β=0, then tanβ=0).

Shadowing is neglected because it was thought by some authors cited by Collado (2009) that blocking has a more pronounced effect on the layout of heliostat fields. Thus, $f_{s\&b} = f_b$.

3. RESULTS AND DISCUSSIONS

In the results section is proposed a study of different heliostat field arrangements for investigating the optical efficiency of solar tower power plants located at low latitudes.

For the model validation, this research compares the results obtained in several simulations with reference values found in the literature for the studied loss mechanisms. Typical values for these mechanisms are found in Tab. 1 (Sattler *et al*., 2015).

Table 1. Typical values of some optical loss mechanisms

Loss mechanisms	Typical efficiencies
Cosine Effect	0.70 – 0.95
Shadowing and Blocking	0.98 – 0.99
Reflectivity	0.80 – 0.95

According to Sattler *et al*. (2015), the total efficiency of the solar field, obtained from Eq. (1) may have values between 45% e 85%. In addition to this general indication, the efficiency found in the simulations was compared with existing plants such as Gemasolar, which presents η = 56% (Collado and Guallar, 2012b).

In the subsection referring to the study of heliostat field arrangements in low latitudes, it is suggested solar tower simulations in Natal, Brazil (S 05° 47' 42" W 35° 12' 32").

To verify which layout is most suitable for plants in low latitudes, two configurations are studied: a southern field, where the heliostats are positioned only to the south side of the tower and a circular field, where the tower is totally surrounded by the heliostats, as shown in Fig. 6.

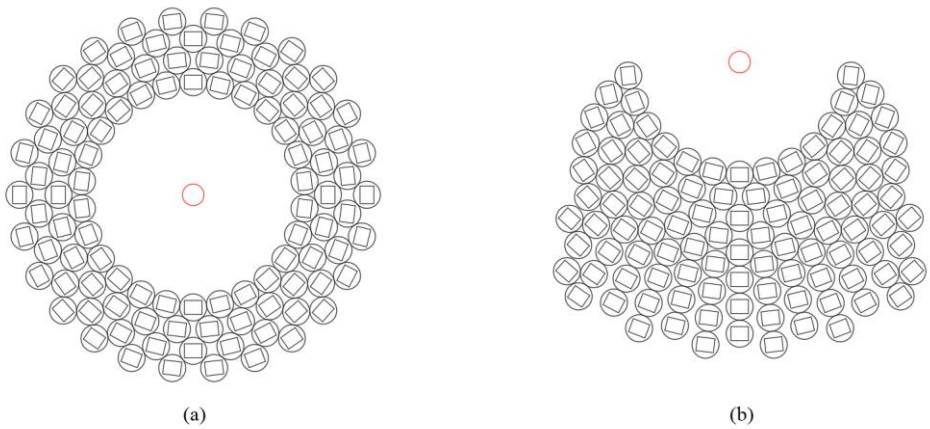

Figure 6. Heliostat field configurations: circular field (a) and southern field (b)

Table 2 shows the main parameters used to design the radial staggered configurations proposed above.

Table 2. Parameters for heliostat field design

Parameter	Value
Tower optical height (THT)	100 m
Number of heliostat	104
Receiver radius (RR)	5 m
Receiver height (RH)	11 m
Heliostat total width (LW)	12.305 m
Heliostat total height (LH)	9.752 m
Heliostat diagonal (DH)	15.7 m
Heliostat total area	120 m²
Effective mirror area	115.7 m²
Aperture area	12,032.8 m²
Security distance (dsep)	3.14 m (0.2 x DH)
Distance from first row to tower (R_1)	78.4 m (0.784 x THT)

To simplify the simulations computational costs, four demonstrative days were chosen to represent a whole year. These days are summer solstice (21st December), autumn equinox (23rd March), winter solstice (21st June) and spring equinox (23rd September). Simulations were performed for the two layouts in the four proposed days, from 06h to 17h00 with an increment of one hour (12 simulations per day). The results for the loss mechanisms ant total field efficiency are shown in Tab. 3.

Table 3. Heliostat field optical efficiencies

	Circular field				Southern field			
	21st Dec	23rd Mar	21st Jun	23rd Sep	21st Dec	23rd Mar	21st Jun	23rd Sep
Reflectivity	0.8360	0.8360	0.8360	0.8360	0.8360	0.8360	0.8360	0.8360
Attenuation	0.9686	0.9686	0.9686	0.9686	0.9640	0.9640	0.9640	0.9640
Cosine effect	0.8365	0.8386	0.8175	0.8392	0.7518	0.8330	0.8774	0.8294
Spillage	0.9994	0.9993	0.9991	0.9993	0.9993	0.9997	0.9999	0.9997
Blocking	0.9939	0.9938	0.9942	0.9937	0.9281	0.9051	0.8931	0.9061
Daily efficiency	0.673	0.674	0.658	0.675	0.564	0.609	0.632	0.607
Annual efficiency	0.670				0.603			

As predicted in the literature, the main mechanisms that influenced the overall efficiency of the heliostats field were reflectivity and cosine effect. As the same mirrors and the same cleaning conditions were used, the reflectivity was the same for both configurations and as described in the Eq. (1), not depend on any variables. For the cosine effect, the circular field presented a 1% greater efficiency than the southern field in the simulations for the proposed days. The atmospheric attenuation was more present in the southern field, which has a lower efficiency since, in this configuration, the average distance between the heliostats and the tower is greater. Due to the proximity between heliostats and tower, spillage losses were insignificant in both cases, when compared to other values. The main divergence between the loss mechanisms of the studied layouts was in blocking efficiency. In this criterion, there was a difference of approximately 9% favorable to the circular field. Fig. 7 shows a comparison between the efficiencies for each loss mechanism in both simulation.

In general, the circular field has achieved an annual efficiency 7% greater than the southern field, being blocking effect, the main divergence factor on the field performance. Analyzing the southern field layout, it has been noted that the radial increment (ΔR) of the last rows is smaller than the front ones, and when this increment is applied in the analytical expression for blocking calculation, this mechanism efficiencies become lower. Empirically, the perception of this effect is trivial, since the closer heliostats rows are arranged, the greater the probability of heliostats in the front to block and to shadow the back ones.

As for model validation, all loss mechanisms presented values within the range presented by the literature, with the exception of the block in the southern configuration, which presented values below those predicted, due to the aforementioned reasons. As a tool to calculate the heliostats field efficiency, the algorithm described in this paper presents some deficiencies, mainly due to the lack of a mathematical model to estimate the effect of shadowing in these plants.

Simulations performed in the software SolarPILOT from National Renewable Energy Laboratory (NREL-USA) for the geographical location proposed in this study, pointed out that this effect is not significant between 09h00 and 15h00, but it has strong influence on the field efficiency at the times close to sunrise and sunset.

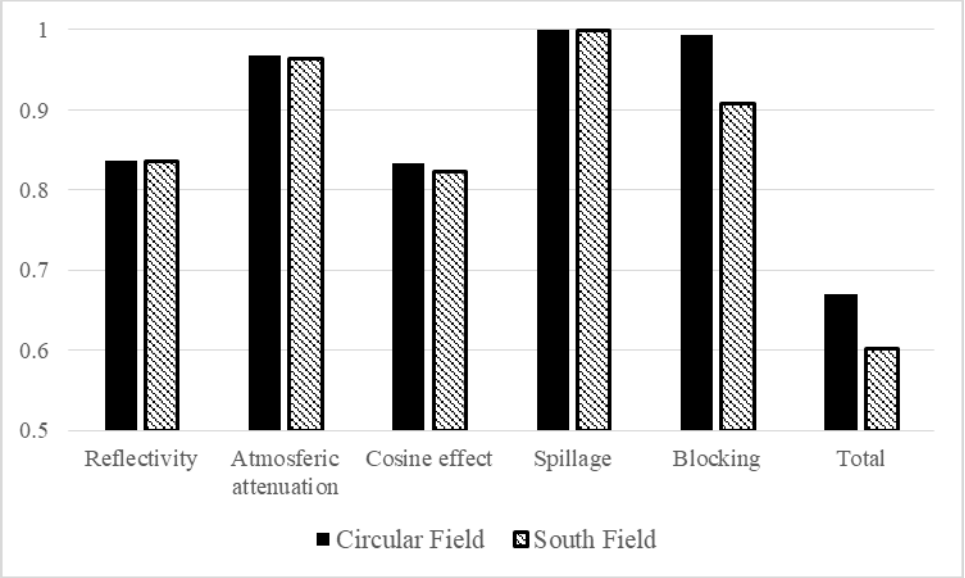

Figure 7. Comparison between loss mechanism efficiencies

Finally, when the efficiencies of the simulated fields in this work were compared to reference efficiency, a difference of up to 11% of the annual value was identified. This difference is due to the dimensions of the simulated layouts, which are smaller than the reference case. Previous works as Collado and Guallar (2012b) has shown that the efficiency of the heliostats closer to the tower is much higher than the rest of the field. In smaller fields, the effect of mechanisms, which depend on heliostat-tower distance (Spillage and Attenuation) are significantly lower.

4. CONCLUSIONS

In this work a MATLAB algorithm was developed to evaluate the performance of heliostat fields in central tower solar plants. This type of algorithm is indispensable in the design of new projects in this area, since, through the use of these programs, it is possible to estimate the efficiency of these plants. From the algorithm developed in this study, the authors intend to implement an intelligent program that returns the best layout for a plant located in an arbitrary location, by evaluating its geographic position and the height of the desired tower.

To calculate the heliostat field efficiency, this algorithm uses different analytical expressions to simulate the optical losses mechanisms of these systems. The code is valid for heliostats and towers with arbitrary position, orientation and size and, although the study object of this paper to be the heliostat field located at low latitudes, the simulations can be performed in any geographical location. The program is very accurate in calculations of the loss mechanisms: cosine effect, atmospheric attenuation, spillage and blocking, but still not be able to model shadowing losses. For future works, the authors intend to develop an efficient method for shadowing losses calculation.

In results, two distinct radial staggered configurations are proposed for simulation at low latitude, a circular layout and a southern layout. Many papers in the literature have performed simulations in one-side layouts (northern field, when located in northern hemisphere, and southern field, when in the southern hemisphere), which have good efficiencies in high latitude locations. This study demonstrated that at low latitudes, circular fields are more feasible than the one-side configuration, presenting 7% higher efficiency in the case study.

The mathematical algorithm presented in this work is interactive and efficient alternative for the study of the loss mechanisms in solar tower power systems, which can make feasible the prospecting new projects for the production of clean energy in Northeast of Brazil, where there are high DNI rates.

5. ACKNOWLEDGEMENTS

This work was supported by the team of Thermal Systems and Alternative Energies Laboratory of the Federal University of Rio Grande do Norte (LSTEA/UFRN).

6. REFERENCES

Barberena, J.G., Mutuberria Larrayoz, A., Sánchez M. and Bernardos A., 2016. "State-of-the-art of heliostat field layout algorithms and their comparison". *Energy Procedia*, Vol. 93, p. 31-38.

Besarati, S.M. and Goswani, D.Y., 2014. "A computationally efficient method for the design of the heliostat field for solar power tower plant". *Renewable Energy*, Vol. 69, p. 226-232.

Blanc, P., Espinar, B., Geuder, N., Gueymard, C., Meyer, R., Pitz-paal, R., Reinhardt B., Renné D., Sengupta M., Wald L. and Wilbert S., 2014. "Direct normal irradiance related definitions and applications : The circumsolar issue". *Solar Energy*, Vol. 110, p. 561–577.

Collado, F.J., 2009. "Preliminary design of surrounding heliostat fields". *Renewable Energy*. Vol. 34, p. 1359-1363.

Collado, F.J. and Guallar, J., 2012a. "Campo: Generation of regular heliostat fields". *Renewable Energy*, Vol. 46, p. 49-59.

Collado, F.J. and Guallar, J., 2012b. "A review of optimized design layouts for solar power tower plants with *campo* code". *Renewable and Sustainable Energy Reviews*. Vol. 20, p. 142-154.

Collado, F.J. and Guallar, J., 2018. "Fast and reliable flux map on cylindrical receivers". *Solar Energy*. Vol. 169, p. 556-564.

Duffie, J.A. and Beckham, W.A., 2013. *Solar Engineering of Thermal Processes*. John Wiley & Sons, New Jersey, 4nd edition.

García, L., Burisch, M. and Sanchez, M., 2015. "Spillage estimation in a heliostats field for solar field optimization". *Energy Procedia*, Vol. 69, p. 1269-1276.

Kistler, B.L., 1986. "*A User's Manual for DELSOL3: A Computer Code for Calculating the Optical Performance and Optimal System Design for Solar Thermal Central Receiver Plants*". Sandia national Laboratories, New Mexico, USA.

Mutuberria, A., Pascual, J., Guisado, M.V. and Mallor, F., 2015. "Comparison of heliostat field layout design methodologies and impact on power plant efficiency". *Energy Procedia*, Vol. 69, p. 1360-1370.

Purohit, I. and Purohit P., 2017. "Technical and economic potential of concentrating solar thermal power generation in India". *Renewable and Sustainable Energy Reviews*, Vol. 78, p. 648-667.

Ramos, A. and Ramos F., 2014. "Heliostat blocking and shadowing efficiency in the video-game era". Cornell University Library. 30 Set. 2017 <https://arxiv.org/abs/1402.1690>.

Sattler, J., O'Connel, B. and Norton, D., 2015. *Advanced CSP teaching Materials*, Chapter 8: Solar Tower Technology. Deutsches Zentrum für Luft- und Raumfahrt – DLR, Germany.

Schmitz, M., Schwarbözl, P., Reiner, B. and Pitz-Paal, R., 2006. "Assessment of the potential improvement due to multiple apertures in central receiver systems with secondary concentrators". *Solar Energy*, Vol. 80, p. 111-120.

Talebizadeh, P., Mehrabian, M.A., Rahimzadeh, R., 2014. "Optimization of Heliostat Layout in Central Receiver Solar Power Plants". *Journal of Energy Enngineering*, Vol. 140.

Wagner, M. J., 2008. *Simulation and Predictive Performance Modeling of Utility-Scale Central Receiver System Power Plants*. Ph.D. thesis, University of Wiscosin – Madison, Madison.

7. RESPONSIBILITY NOTICE

The authors are the only responsible for the printed material included in this paper.